JVSTA Journal of Vacuum Science & Technology A

Evaluation of electropolished stainless steel electrodes for use in DC high voltage photoelectron guns

Mahzad BastaniNejad, Abdelmageed A. Elmustafa, Eric Forman, Steven Covert, John Hansknecht, Carlos Hernandez-Garcia, Matthew Poelker, Lopa Das, Michael Kelley, and Phillip Williams

Citation: Journal of Vacuum Science & Technology A **33**, 041401 (2015); doi: 10.1116/1.4920984
View online: http://dx.doi.org/10.1116/1.4920984
View Table of Contents: http://scitation.aip.org/content/avs/journal/jvsta/33/4?ver=pdfcov
Published by the AVS: Science & Technology of Materials, Interfaces, and Processing

Evaluation of electropolished stainless steel electrodes for use in DC high voltage photoelectron guns

Mahzad BastaniNejad[a] and Abdelmageed A. Elmustafa
Department of Mechanical Engineering, Old Dominion University, Norfolk, Virginia 23529

Eric Forman, Steven Covert, John Hansknecht, Carlos Hernandez-Garcia, and Matthew Poelker
Thomas Jefferson National Accelerator Facility, Newport News, Virginia 23606

Lopa Das and Michael Kelley
The College of William & Mary, Williamsburg, Virginia 23187

Phillip Williams
NASA Langley, Hampton, Virginia 23681

(Received 28 April 2015; accepted 28 April 2015; published 15 May 2015)

DC high voltage photoelectron guns are used to produce polarized electron beams for accelerator-based nuclear and high-energy physics research. Low-level field emission (∼nA) from the cathode electrode degrades the vacuum within the photogun and reduces the photoelectron yield of the delicate GaAs-based photocathode used to produce the electron beams. High-level field emission (>μA) can cause significant damage the photogun. To minimize field emission, stainless steel electrodes are typically diamond-paste polished, a labor-intensive process often yielding field emission performance with a high degree of variability, sample to sample. As an alternative approach and as comparative study, the performance of electrodes electropolished by conventional commercially available methods is presented. Our observations indicate the electropolished electrodes exhibited less field emission upon the initial application of high voltage, but showed less improvement with gas conditioning compared to the diamond-paste polished electrodes. In contrast, the diamond-paste polished electrodes responded favorably to gas conditioning, and ultimately reached higher voltages and field strengths without field emission, compared to electrodes that were only electropolished. The best performing electrode was one that was both diamond-paste polished and electropolished, reaching a field strength of 18.7 MV/m while generating less than 100 pA of field emission. The authors speculate that the combined processes were the most effective at reducing both large and small scale topography. However, surface science evaluation indicates topography cannot be the only relevant parameter when it comes to predicting field emission performance. © *2015 American Vacuum Society*.
[http://dx.doi.org/10.1116/1.4920984]

I. INTRODUCTION

One of the limiting factors of direct current (DC) high voltage photoelectron guns is low-level field emission (∼nanoAmperes, nA) from the cathode electrode which degrades the vacuum within the gun via electron stimulated desorption of gas. Under degraded vacuum conditions, the photocathode yield—or quantum efficiency (QE)—diminishes more quickly due to ion bombardment, the mechanism whereby ions produced by the photoemitted beam are accelerated toward the photocathode. These ions may sputter away the chemicals used to reduce the work function at the surface of the photocathode, or they may penetrate the surface and serve as trapped interstitial defects that reduce the electron diffusion length. The QE of the photocathode can be restored, but this introduces costly accelerator downtime. Higher levels of field emission (∼microAmperes, μA) can heat flange joints creating vacuum leaks. At hundreds of microAmperes, field emission can lead to serious damage of insulators and electrodes. For these reasons, the onset of field emission determines the acceptable operating voltage of the photogun, often restricting operation to voltages significantly below the desired value required for optimized electron beam parameters. This is especially true for today's photoelectron gun projects aimed at operating at 350 kV DC and higher,[1–6] where eliminating field emission is one of the key technological challenges.

Field emission often originates from microprotrusions and particulate contamination on the surface of the cathode electrode, which serves to enhance the localized electric field.[7] Electrode surface preparation is an essential step during the construction of the photoelectron gun. It is common to polish the electrodes to mirrorlike surface finish using silicon carbide paper and diamond paste of successively finer grit. Diamond-paste polishing is a laborious process requiring strict adherence to the protocol,[8] with prevailing wisdom suggesting that pressing too hard on the piece leads to microscopic tips that become "rolled over," and trapping particulate contamination. As a result, the performance of one diamond-paste polished electrode can be very different from that of another that was polished, for example, by another person. There is strong interest in developing polishing

[a]Electronic mail: Mahhzad@gmail.com

procedures that provide consistent and favorable results, and ideally, requiring less time and labor.

An alternative approach to altering the surface topography of metals is electropolishing. As a practical art, electropolishing has been used since the 1930s. The consensus fundamental understanding was solidified in the 1980s and is exemplified by the work of the Landolt group.[9] These principles have been applied at our institute to obtain unprecedentedly smooth interior surfaces on niobium superconducting radio frequency accelerator cavities.[10,11] We were therefore encouraged to begin experiments on stainless steel photoelectron gun electrodes.

Previous applications of electropolishing to particle accelerators include processing the internal surface of vacuum chambers and thereby reducing the gas load that stems from hydrogen outgassing.[12,13] At least one group has tested electropolished electrodes inside DC high voltage photoelectron guns, reaching bias voltages exceeding 500 kV.[14] This impressive voltage metric was reached using a combination of current conditioning, and helium gas conditioning, with field emission levels reduced to sufficiently low levels to support beam delivery at 400 kV using an alkali-antimonide photocathode. It is unknown if field emission levels were low enough to support sustained beam delivery using a delicate GaAs photocathode. Williams and Williams[13] evaluated the relative effectiveness of different polishing techniques including machining, mechanical polishing and electropolishing. They found mechanical polishing to be the most reliable technique providing the lowest and most stable field emission current. In 1985, Gruszka and Moscicka-Grzesiak investigated the effects of current conditioning on electropolished stainless steel, aluminum and copper electrodes.[15] They discovered that the emission current depends on the type of metal and the surface roughness of the electrodes and that the optimum conditioning current has a greater value for smoother electrode surfaces. In this work, the field emission characteristics of electropolished and diamond-paste polished electrodes were evaluated in a test stand capable of operation at −225 kV and field strength ∼18.7 MV/m.

II. EXPERIMENT

A. Materials and methods

Five electrodes were manufactured from 304L and 316L stainless steel and cut to shape using hydrocarbon-free lubricants to obtain a 32 μ in. RMS surface finish. Each Pierce-type electrode (6.35 cm dia., 2.85 cm thick) was identical to electrodes used inside a DC high voltage photoelectron gun in operation at the Continuous Electron Beam Accelerator Facility at Jefferson Lab.[16]

Diamond-paste polishing[9] is a conventional polishing technique employed for many years, particularly for electrodes used in DC high voltage photoelectron guns. For our experiment, electrodes were polished on a potter's wheel, first with silicon carbide paper of increasingly finer grit (300 and then 600 particles/in.^{2}) followed by polishing with diamond grit (6 μm and then 3 μm). Between each polishing step, the electrode was cleaned in an ultrasonic bath using an alkali solution. The end result was an electrode with mirror-like surface finish. The nominally identical diamond-paste polished electrodes are referred to as DPP1, DPP2, and DPP3.

An extensive literature about electropolishing of stainless steel exists; many processes are available. As a beginning point for our research, it made the most sense to use the conditions widely applied to accelerator vacuum system components, recognizing that these might not be the best eventual choice. For this work, the electrodes were electropolished by an experienced commercial vendor,[17] using a proprietary process, but one considered being relatively generic in terms of technique. Per the vendor's assessment, electropolishing resulted in the removal of approximately 10 μm of material from the surface. Three stainless steel cathode electrodes with different initial surface roughness were electropolished. One electrode was electropolished immediately following machining, one after mechanical polishing with silicon carbide paper (300 and 600 particles/in.^{2}), and one after silicon carbide polishing (300 and 600 particles/in.^{2}) followed by diamond-paste polishing (6 and 3 μm grit). The electropolished electrodes are referred to as EP1, EP2, and EP3, respectively. Electrode EP3 was first evaluated as diamond-paste polished electrode DPP3. After initial evaluation as DPP3, it was electropolished and renamed EP3. Since the electropolishing process was expected to remove a 10 μm surface layer, we expected this electrode to exhibit characteristics independent of its previous state. We will discuss this assumption in further detail, below.

B. High voltage apparatus

Cathode electrodes were suspended from a tapered conical insulator that extended into the ultrahigh vacuum test chamber (Fig. 1). A single stainless steel (304L) anode was used for all measurements, and consisted of a polished flat plate with a Rogowski edge profile that was electrically isolated from ground through a sensitive current meter (Keithley electrometer model 617). The anode could be moved up or down to vary the cathode-anode gap and therefore the field strength.

Prior to the application of high voltage, the entire vacuum apparatus was baked at 200 °C for 30 h to achieve vacuum level in the 5×10^{-11} Torr range. Every effort was made to keep the vacuum conditions consistent from sample-to-sample. A full description of the test apparatus can be found in Ref. 18.

Electrodes were first *current conditioned*,[7] a technique where voltage is applied in small incremental steps with the objective to minimize field emission in a controllable manner. However, current conditioning is a delicate, lengthy, and unpredictable method that occasionally results in high voltage breakdown, leading to electrode and insulator damage.

Following meticulous current conditioning, electrodes were *gas conditioned*,[7,18] a technique where inert gas is introduced into the vacuum chamber while the cathode electrode is biased at voltages high enough to produce field emission. Field emitted electrons ionize the gas; the ions are then

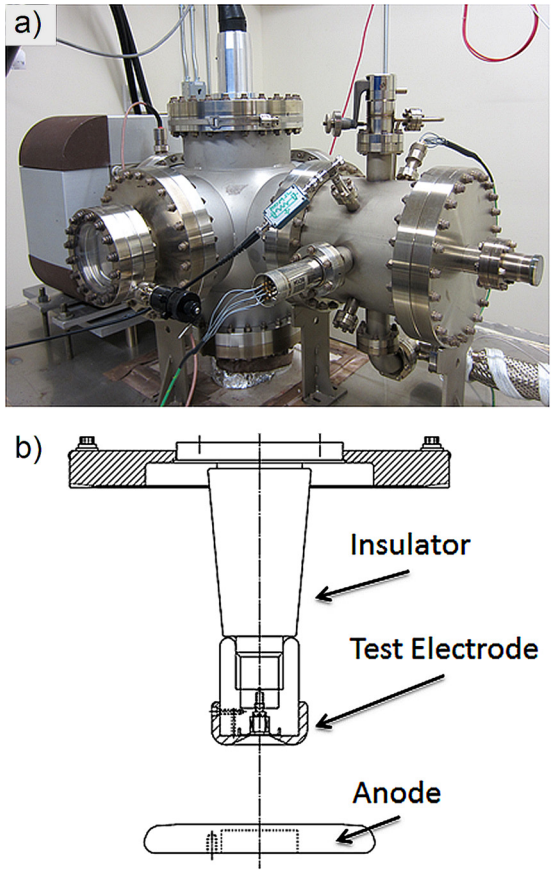

FIG. 1. (Color online) (a) Photograph of the DC high voltage field emission test stand used to evaluate each cathode electrode; (b) a schematic view of the insulator (12.7 cm long), test electrode (6.35 cm diameter); and anode (15.24 cm diameter) used to collect the field emission.

accelerated by the electrostatic potential toward the cathode electrode drastically reducing field emission. Two gasses with distinctly different atomic mass were used in these experiments, helium and krypton, at $\sim 1 \times 10^{-5}$ Torr, for 20 min intervals. The nonevaporable getters inside the vacuum apparatus do not pump inert gasses: therefore, when the supply of gas was terminated, the vacuum recovered to a level nearly the same as before gas conditioning within 24 h. Sometimes field emission reduction was observed in just one implementation of gas conditioning, while in other instances, multiple conditioning cycles were required to observe significant reduction in field emission. Gas conditioning was halted after 20–30 min or after a sudden reduction of field emission current in order to measure the new field emission status of the surface.

High voltage evaluation of electrodes involved monitoring the vacuum level via the ion pump current, the x-ray radiation using Geiger counters placed around the apparatus, and the anode current while increasing the applied voltage. High voltage was first applied to the electrode using the largest cathode–anode gap of 50 mm where the maximum field strength reaches 13 MV/m at −225 kV bias. The gap was then decreased to achieve higher field strength. The smallest gap used for these tests was 20 mm and provided maximum field strength of ∼18.7 MV/m when the cathode was biased at −225 kV. Smaller gaps provided significantly higher field strength, but often resulted in catastrophic electrode damage. Therefore, the voltage was adjusted to limit field emission current to a few nanoAmperes in the current conditioning phase and to a few microAmperes during gas conditioning.

III. EXPERIMENTAL RESULTS

Field emission current (I) versus applied voltage (V) is shown in Fig. 2, for both groups of electrodes, before and after gas conditioning. The results for electropolished electrodes are displayed on the left, and on the right for diamond paste-polished electrodes. For electrodes that generated sufficiently high levels of field emission, fits were applied to the data using the Fowler–Nordheim equation, discussed below. The field emission performance of the entire group of electrodes was very random before gas conditioning. In general, the electropolished electrodes exhibited less field emission before gas conditioning, compared to the diamond paste polished electrodes (despite large variations in surface roughness, as will be presented below). However, all of the diamond-paste polished electrodes improved significantly following gas conditioning, achieving comparable performance and showing no field emission at −225 kV at the 50 mm gap. Interestingly, inert gas conditioning with helium or krypton did very little to improve the performance of the electropolished electrodes, and in the case of EP1, actually served to degrade performance.

Table I lists the field strength at which each electrode produced 100 pA of field emission for anode–cathode gaps between 20 and 50 mm. Field strength values were estimated using the field mapping program POISSON.[19,20] The value 100 pA was chosen because it was large enough to accurately apply a Fowler–Nordheim fit to the data. Before gas conditioning, some electropolished electrodes reached higher field strengths before field emitting, compared to diamond-paste polished electrodes. Averaged over all gaps, the onset of field emission for electropolished electrodes occurred at 11.5 MV/m compared to 7.1 MV/m for diamond paste polished electrodes. However, after gas conditioning, the diamond-paste polished electrodes improved significantly, reaching field strengths near ∼13 MV/m or higher, without field emission, whereas the performance of the electropolished electrodes was either unchanged, or exhibited small improvement or degradation. The best performing electrode (EP3) was one that was both diamond-paste polished and electropolished, reaching a field strength of 18.7 MV/m while generating less than 100 pA of field emission.

IV. DISCUSSION

A. Materials and methods

After high voltage evaluation, the topography of all electrodes was examined by optical profilometry and by atomic force microscopy (AFM) of replicas. The results of optical profilometry[21] (NT1100 optical profilometer) are presented as false-color images in Fig. 3. An optical profilometer does not contact the surface of the specimen under investigation. It provides a measure of two quantities, roughness and

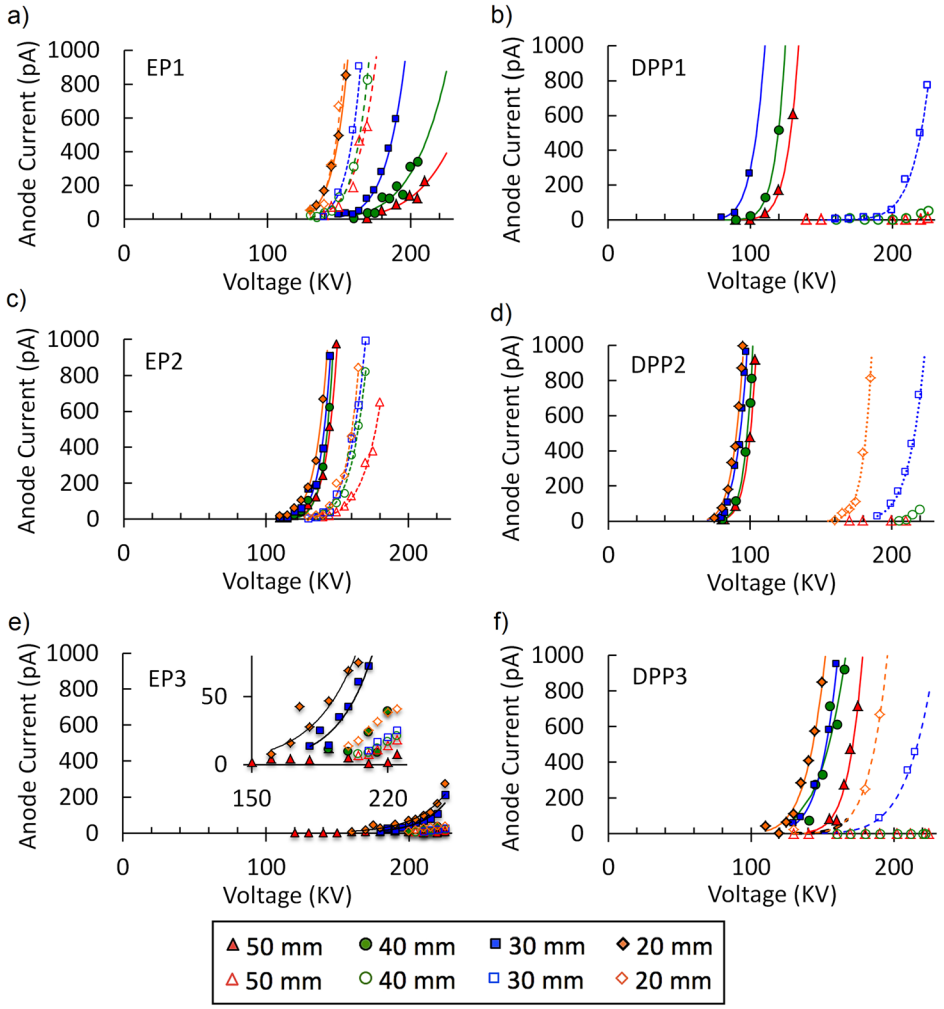

FIG. 2. (Color online) Field emission current (I) vs applied voltage (V) is shown in I to V curves for electropolished electrodes [(a), (c), and (e)] and diamond-paste polished electrodes [(b), (d), and (f)]. Solid lines and closed markers represent results before gas conditioning; dashed lines and open markers represent results postgas conditioning. The lines represent fits to the data using the Fowler–Nordheim equation. For samples that exhibited very low levels of field emission, fits were not possible, and were omitted. For each data point, the field emission current was averaged over a period of minutes, resulting in error bars comparable to the size of the symbols used in the plots.

TABLE I. Field strength (MV/m) at which each electrode exhibited 100 pA of field emission at different gaps before (top) and after (bottom) gas conditioning for electropolished and diamond paste polished electrodes. For entries with (>) symbol, field emission current did not exceed 100 pA at −225 kV, and consequently, the field strength must exceed the maximum value provided by the high voltage power supply.

Turn on field strength (MV/m) at 100 pA, before gas processing vs gaps

Gap (mm)	EP1	EP2	EP3	DPP1	DPP2	DPP3
50	10.9	7.3	>12.6	6.4	4.9	8.7
40	11.1	8.1	>13.8	6.6	5.4	8.1
30	11.4	8.7	14.8	6.2	5.5	9.1
20	11.3	10.5	17.5		6.6	10.5

Turn on field strength (MV/m) at 100 pA, after gas processing vs gaps

Gap (mm)	EP1	EP2	EP3	DPP1	DPP2	DPP3
50	8.2	9.2	>12.6	>12.6	>12.6	>12.6
40	9.1	9.9	>13.8	>13.8	>13.8	>13.8
30	9.8	10.5	>15.1	13.6	13.5	12.9
20	11.3	12.8	>18.7		14.4	14.1

waviness, which describe the RMS magnitude of peak-to-valley surface variations measured over fine and coarse scales, respectively. These quantities are discerned by applying different spatial filtering to the same data file. Specifically, roughness (waviness) provides a measure of RMS surface variation occurring at spatial frequencies greater than (less than) 3×10^{-5} cycles/nm.

Each image shows a portion of the electrode ($\sim 500 \times 500\ \mu$m) in the vicinity of the region exposed to the highest field strength, and therefore the region most likely to produce field emission. The images in the top row correspond to diamond-paste polished electrodes and the bottom row shows images of electropolished electrodes. Quantitative results are presented in Table II. Overall, the electropolished-only electrodes exhibit higher levels of roughness and waviness compared to diamond-paste polished electrodes. Surprisingly, the electrode polished with silicon carbide paper before electropolishing (EP2), possessed comparable surface features as the electrode that was electropolished without any preparatory mechanical polishing (EP1). The

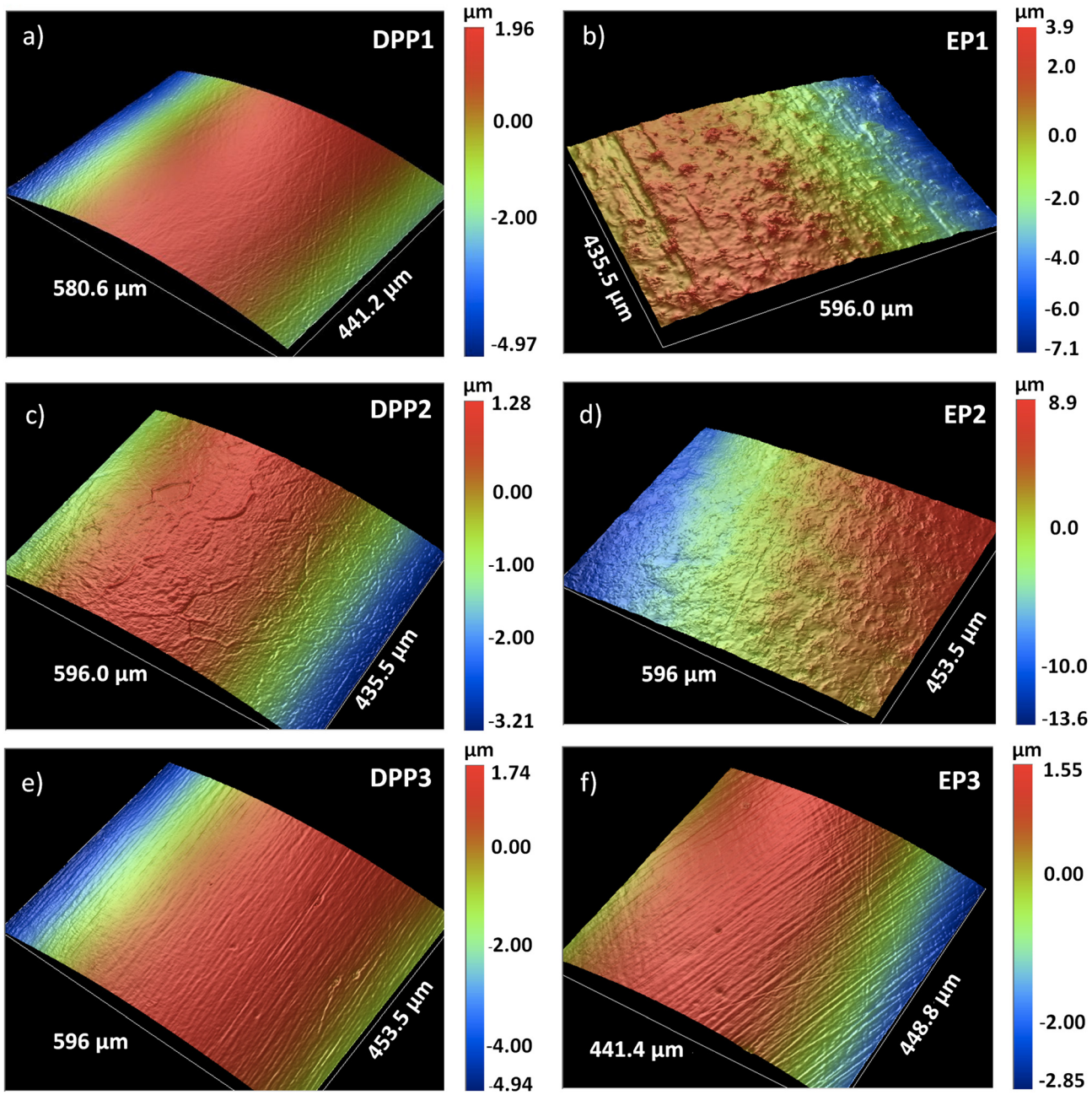

FIG. 3. (Color online) False-color optical profilometer images of the electrodes showing regions in the vicinity of the highest field strength for diamond-paste polished electrodes [(a), (c), and (e)] and electropolished electrodes [(b), (d), and (f)]. Specific details of each electrode are described in the text.

electrode that was diamond-paste polished (DPP3) and then electropolished (EP3) exhibited topographical features nearly indistinguishable from DPP electrodes. But when evaluated using a different technique, described below, electropolishing was observed to roughen the surface of EP3 at low spatial frequencies.

TABLE II. Surface variations of all six electrodes measured using an optical profilometer, on a fine and coarse scale. Roughness (waviness) provides a measure of RMS surface variation occurring at spatial frequencies greater than (less than) 3×10^{-5} cycles/nm. Electrode EP3 was originally electrode DPP3.

	EP1	EP2	EP3	DPP1	DPP2	DPP3
Waviness (nm)	312	385	76	25	30	73
Roughness (nm)	163	140	37	11	29	31

Optical profilometry provides a useful measure of fine and coarse scale roughness; however, there is a level of subjectivity associated with this evaluation technique, due to spatial filtering software that can be adjusted by the user.

AFM assesses topography to a smaller dimensional scale than optical profilometry, but the instruments available at Jefferson Lab cannot accommodate a complete electrode. Instead, replicas from the high-field areas were collected and examined. The procedure has been reported previously.[22] Briefly, cellulose acetate replicating tape is softened in acetone, applied to the electrode surface and let to dry. AFM operation must take account of lower modulus of the

polymer. We used a Digital Instruments "Dimension 3100" AFM with a Nanoscope IV controller, with tips having a 75 kHz resonant frequency and force constant of 3 N/m. The replicas were scanned as $50 \times 50\ \mu$m areas (100 nm resolution) at four different locations on each sample. The data were analyzed in terms of power spectral density (PSD) as described in Ref. 23.

The AFM data were used to calculate PSD results presented in Fig. 4. The notable feature is that the topography contribution from a dimensional scale of near-micron and greater was at least one order of magnitude greater for the EP than for the DPP electrodes, as indicted by the data points in the upper left corner of the graph. This agrees with the generalized trend of the optical profilometry results.

B. Fowler–Nordheim line-plot analysis

The Fowler–Nordheim equation successfully describes the observed "prebreakdown" functional form of field emission from a single emitter[6]

$$I = J \cdot A_e = C_1 A_e \beta^2 E^2 e^{-C_2/\beta E}, \tag{1}$$

where I is the field emission current in A, J is the field emission current density, A_e is the area of the field emitter in units of m^2, E is the average surface field strength (MV/m), β is the field enhancement factor defined as the ratio of the emitter electric field to the average surface field, and factors C_1 and C_2 are fundamental constants given by

$$C_1 = \frac{1.54 \times 10^{-6} \times 10^{4.52.\phi^{-0.5}}}{\phi}, \tag{2}$$

$$C_2 = 6.53 \times 10^9 \phi^{1.5}, \tag{3}$$

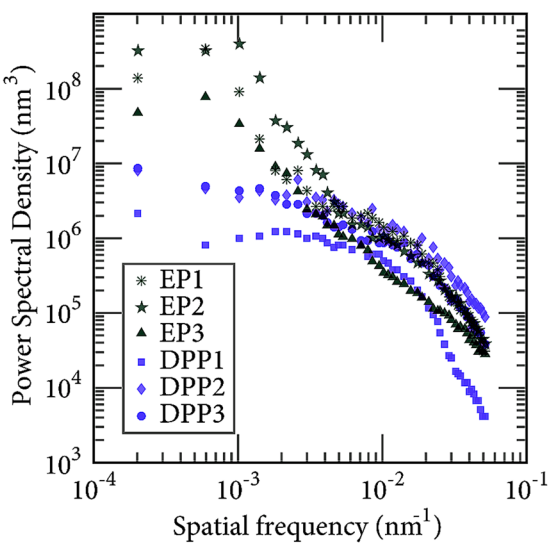

FIG. 4. (Color online) Power spectral density plots of six electrodes: three electropolished and three diamond-paste polished. The graph provides a measure of surface feature variation as a function of spatial frequency. The diamond-paste polished electrodes have smooth surfaces at low spatial frequencies, compared to the electropolished electrodes.

the term φ is the work function (eV) of the material, typically assumed to be ~4.5 eV for most electrode materials.

It is common to replot I-V curves like those in Fig. 2 as Fowler–Nordheim line plots, showing the variation of the quantity $\log(I/E^2)$ as a function of $1/E$. Such a representation can be used to estimate the field enhancement factor, β, and the field emission emitter area, A_e, using the expressions below:[8]

$$\text{Slope} = \frac{d\left(\log_{10} I/E^2\right)}{d(1/E)} = -\frac{2.84 \times 10^5 \phi^{1.5}}{\beta}, \tag{4}$$

$$\text{Intercept} = \text{Log}_{10}(I_F/E^2)_{E\to\infty} = \text{Log}_{10}\left[\frac{1.54 \times 10^{-6} A_e \beta^2 \times 10^{4.52\phi^{-0.5}}}{\phi}\right]. \tag{5}$$

As illustrated in Table III, gas conditioning yielded smaller field enhancement factors and larger emitter areas for each electrode, suggesting that field emitter tips became blunted and wider as a result of gas conditioning. The change in β and A_e values after gas conditioning was much larger for the diamond-paste polished electrode compared to electropolished electrodes. For diamond-paste polished electrodes, the average value of β reduced from 558 to 201, and the calculated emitting area increased from an average value of 3.6×10^{-19} to 2.7×10^{-17} m^2. For the electropolished electrodes, the average value for the field enhancement factor, β, reduced from 466 to 410, and the calculated emitting area had only a small change from an average value of 6.8×10^{-19} to 1.2×10^{-18} m^2.

Noting also that β can be described as the ratio of the emitter height to emitter radius, the Fowler–Norheim line plot analysis can be used to estimate the topography of the field emitter. Emitter heights calculated in this manner are shown in Table III, and these values can be compared to optical profilometer measurements summarized in Table II. For electropolished electrode samples EP1 and EP2, there is reasonable agreement between the two assessments, with calculated emitter heights and measured roughness/waviness values of the order 200–400 nm. But for electropolished electrode sample EP3, the Fowler–Nordheim line plot analysis suggests a much smaller emitter height compared to measured topography: a few nanometers compared to tens of nanometers, respectively. For the diamond-paste polished electrodes, there is consistency between the two assessment techniques only for sample DPP3, with calculated emitter height and measured topography on the order of tens of nanometers. For samples DPP1 and DPP2, the Fowler–Nordheim line plot analysis suggests much larger emitter heights than measured via optical profilometry. Moreover, this traditional Fowler–Nordheim line plot analysis reveals the counterintuitive trend of increasing emitter heights following gas conditioning.

It should be mentioned that field emission from large area electrodes likely originates from multiple emitters, whereas Eqs. (4) and (5) were derived for a single emitter. Some researchers question the validity of the Fowler–Nordheim

TABLE III. Summary of Fowler–Nordheim line plot analysis: field enhancement factor, β, and emitting area, A_e, before and after gas conditioning. The statistical variations in the values listed below are small, with chi-squared fit parameters close to unity. More significant are the large systematic variations between different electrodes, which point to the unpredictable nature of field emission, and challenges associated with preparing identical electrode samples. Emitter heights were estimated by noting that β can be described as the ratio of the emitter height to emitter radius. Values in bold are consistent with topographical features derived via optical profilometry, and shown in Table I. The right-most column indicates the change in work function required to explain improved performance following gas conditioning, assuming the field enhancement factor β remained constant.

Electrodes	β, pregas conditioning	β, postgas conditioning	A_e (m^2), pregas conditioning	A_e (m^2), postgas conditioning	Emitter height (nm), pregas conditioning	Emitter height (nm), postgas Conditioning	Work function (eV)
EP1	413	413	1.2×10^{-18}	1.2×10^{-18}	**255**	**255**	4.4
EP2	485	362	8.5×10^{-19}	2.4×10^{-18}	**252**	**316**	5.3
EP3	501	456	5.3×10^{-23}	1.2×10^{-22}	2	2.8	4.7
DPP1	228	134	9.7×10^{-19}	1.1×10^{-17}	127	250	6.3
DPP2	972	299	8.4×10^{-20}	7.1×10^{-17}	159	1422	9.7
DPP3	475	171	2.5×10^{-20}	1.4×10^{-19}	**42**	**36**	8.7

line plot analysis for large area electrodes, describing the values of β and A_e as a "distribution" of values.[24] Another criticism of the traditional Fowler–Nordheim line plot analysis relates to the assumption that the work function, φ, remain a constant value.[6,25,26] This is highly unlikely, especially following gas conditioning where implanted ions can increase the work function, and considering that field emitters are often associated with unknown impurities of various chemical compositions. With these criticisms of the Fowler–Nordheim line plot analysis in mind, the postgas conditioning I-V curves shown in Fig. 2 were replotted as Fowler–Nordheim line plots, but considering the work function, φ, and emitter area, A_e, as variables, and assuming the field enhancement factor β remained constant, before and after gas conditioning. The goal of this exercise was to determine the extent the work function must vary, to explain the improved postgas conditioning performance. Not surprisingly, since gas conditioning was largely ineffective for the electropolished electrodes, the work function remained relatively unchanged and near the widely assumed value of 4.4 eV (Table III). For the diamond-paste polished electrodes, the work function would need to increase significantly, by multiplicative factors ranging from 1.4 to 2.2, to explain the improved performance following gas conditioning. It seems unlikely that the work function could increase by so much.[27] All of these considerations point to the complex nature of field emission, both in terms of its origins and the many mechanisms that can alter field emission behavior.

C. How ions interact with the electrode surface

The software program TRIM (TRANSPORT OF IONS IN MATTER)[28] was used to help gain insight into how inert gas ionized by field emission, interacts with the electrode surface, and specifically, to help explain the observation that gas conditioning (at least how it was implemented) did little to improve the performance of the electropolished electrodes. In previous experiments, we have studied the effect of gas conditioning in reducing field emission via two mechanisms: blunting of emission sites by sputtering, and the increase of the work function by ion implantation.[18] Figure 5 shows the TRIM simulation results for helium and krypton ion implantation as a function of angle of incidence for various ion energies, where 0° corresponds to ions striking the electrode normal to the surface. Specifically, Fig. 5 shows the mean value of the distribution of implanted ions, based on simulations using 10 000 ions incident at various energies and angles. For both gas species, simulation results indicate significantly fewer ions implanted at large angles of incidence, i.e., a condition representative of a rough surface, suggesting that the typical 20 min application of gas conditioning may have been insufficient to significantly increase the work function of the electropolished electrode surface.

Figure 6 shows TRIM simulations of ion sputtering from stainless steel versus the angle of incidence, for both helium and krypton. To generate this plot, an ion energy of 0.2 keV

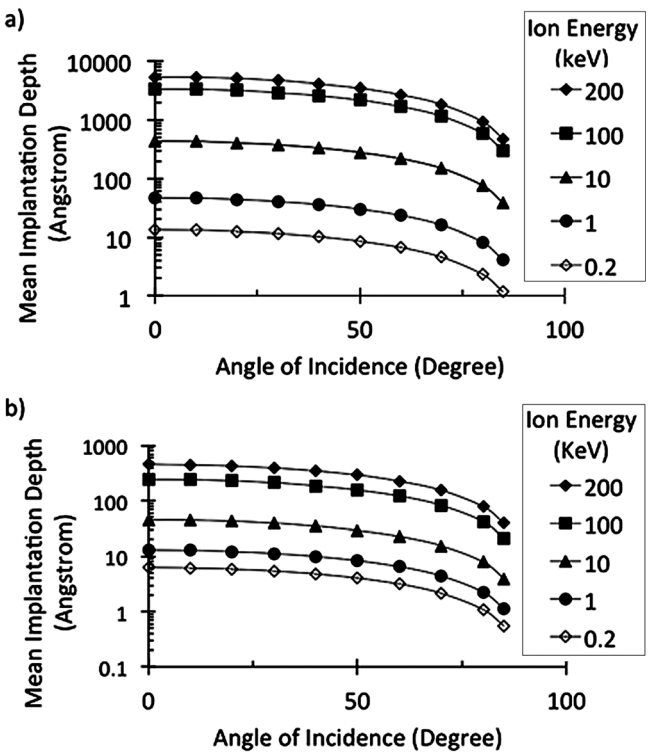

FIG. 5. (a) Number of helium ions implanted within a stainless steel surface as a function of angle of incidence, with 0° representing an ion striking the surface at normal incidence; (b) a similar plot for krypton ions. Significantly fewer ions are implanted at large angles, representative of rough surfaces.

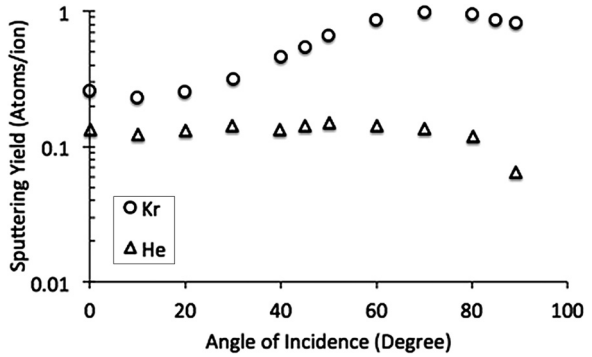

FIG. 6. Sputtering yield from stainless steel vs the angle of incidence for helium and krypton at 0.2 keV energy.

was used, which corresponds to the ion energy where the sputtering yield for both gas species are closest in magnitude, at normal incidence. For helium ions, the sputtering yield is relatively constant as a function of angle of incidence and one order of magnitude smaller than for krypton. The sputtering yield for krypton is maximum at an angle of incidence of 70°. As a result, sputtering from recesses in a rough surface (where contamination could reside) will be less efficient, because adjacent surface peaks restrict access to only small angles where the sputtering yield is approximately five-times smaller. Although krypton sputtering of the emitter tips is enhanced at large angles of incidence, it is possible that gas conditioning was not performed long enough to significantly blunt the emitter tips of the comparatively rough electropolished surfaces.

V. SUMMARY AND CONCLUSIONS

Electropolished electrodes exhibited less field emission upon initial application of high voltage, but showed less improvement with gas conditioning compared to the diamond-paste polished electrodes. In contrast, the diamond-paste polished electrodes responded favorably to gas conditioning, and ultimately reached higher voltages and field strengths without field emission, compared to electrodes that were only electropolished. However, the best performing electrode was one that was both diamond-paste polished and electropolished, reaching a field strength of 18.7 MV/m while generating less than 100 pA of field emission. It is possible this electrode performed best because it was high voltage conditioned twice, retaining benefits incurred by current and gas conditioning when it was diamond-paste polished sample DPP3. However, the authors think this is unlikely because the electropolishing process was reported to have removed 10 μm of material, and since most helium ions are implanted at depths less than 1 μm.[19] Furthermore, the implanted ions would diffuse from the surface during the bakeout of the vacuum apparatus when the electrode was reinstalled in its new state. It seems more plausible that the electropolishing process provided an unexpected benefit, beyond the initial assumption that it served to create a smooth surface. For example, electropolishing also could have served to increase the work function of the material. Future work must be performed to validate this speculation.

The surface characterization techniques utilized for this work support the generalized correlation between electrode surface roughness and high voltage performance, providing some degree of predictability. That is, a smooth electrode (one with small waviness values, and small PSD values at lower spatial frequencies) will generally exhibit lower levels of field emission following proper conditioning at high voltage. However, topography cannot be the sole determining factor that predicts an electrode's high voltage performance, as evidence by the electrode that was both diamond-paste polished and electropolished. It had topographical features indistinguishable from electrodes that were only diamond-paste polished, and yet, it performed significantly better than all of the other electrodes. Conversely, the smoothest electrode, one that was only diamond-paste polished, had performance comparable to the other diamond-paste polished electrodes. In addition, the traditional Fowler–Nordheim line-plot analysis inferred rather coarse topographical features for diamond-paste polished electrodes known to be very smooth. All of these interesting observations suggest topography is not the only relevant issue influencing an electrode's field emission characteristics. Further studies should be performed to better appreciate the specific benefit provided by electropolishing an already smooth surface; in particular studies that directly measure the surface work function would be very informative, helping to disentangle some of these questions.

Simulation results suggest there is significantly less ion implantation during gas conditioning on rough surfaces compared to smooth surfaces. Although sputtering yield from krypton is actually enhanced for rough surfaces, it is possible that the gas conditioning as implemented in this work was not performed long enough to sufficiently blunt the field emitter tips with larger area in the electropolished electrodes. This speculation is supported by Maxson *et al.*[14] that describes successful high voltage conditioning of electropolished electrodes biased at voltages exceeding 500 kV. Helium gas conditioning was credited to have helped reduce field emission, but it was employed for hours-long periods, whereas our gas conditioning cycles totaled just 1 h duration.

Our observations indicate that electropolishing alone, by conventional commercial methods, does not produce an electrode that outperforms an electrode polished via the labor-intensive diamond grit procedure. However, our work does not preclude the possibility of refining the electropolishing technique, either by using different recipes or by using it together with mechanical polishing, to attain smoother electrodes and consequently less field emission at high voltages required by DC photoelectron guns.

ACKNOWLEDGMENTS

Authored by Jefferson Science Associates under U.S. DOE Contract No. DE-AC05-84ER40150 and with funding from the DOE Office of High Energy Physics and the Americas Region ILC R&D program. The U.S. Government retains a nonexclusive, paid-up, irrevocable, world-wide

[1]R. Hajima and R. Nagai, Nucl. Instrum. Methods Phys. Res. A **557**, 103 (2006).
[2]C. Hernandez-Garcia *et al*., *Proceedings of the ERL09*, Ithaca, NY (2009), p. 37.
[3]L. B. Jones, S. P. Jamison, Y. M. Saveliev, K. J. Middleman, and S. L. Smith, AIP Conf. Proc. **1149**, 1084 (2009).
[4]B. M. Dunham and K. W. Smolenski, *IEEE International Conference on Power Modulator and High Voltage*, Atlanta, GA (2010), pp. 98–101.
[5]N. Nishimori *et al*., AIP Conf. Proc. **1149**, 1094 (2009).
[6]R. V. Latham, *High Voltage Vacuum Insulation*, 2nd ed. (Academic, London, 1995).
[7]J. J. Francis, "SLC procedural note," FP-238-042-94 (1991) and modifications described in University of Illinois, Champaign, IL 1991; B. Dunham, "Notes on diamond paste polishing of stainless steel," Nuclear Physics Laboratory Technical Notes, 19 May 90 revised 23 July 92, University of Washington, Seattle, WA, 1992.
[8]D. Landolt, Electrochim. Acta **32**, 1 (1987); D. Landolt, P. F. Chauvy, and O. Zinger, *ibid*. **48**, 3185 (2003).
[9]R. Geng, G. Ciovati, and C. Crawford, *Proceedings of the 14th International Conference on RF Superconductivity*, Berlin, Germany, 25–27 September 2009 (HZB-Berichte, Berlin, 2009), p. 370.
[10]H. Tian, S. G. Corcoran, C. E. Reece, and M. J. Kelley, J. Electrochem. Soc. **155**, D563 (2008).
[11]*Foundations of Vacuum Science and Technology*, edited by J. Lafferty (John Wiley and Sons Inc., Canada, 1998) and references within.
[12]Y. Tito Sasaki, J. Vac. Sci. Technol. A **25**, 1309 (2007).
[13]D. W. Williams and W. T. Williams, J. Phys. D: Appl. Phys. **5**, 1845 (1972).
[14]J. Maxson, I. Bazarov, B. Dunham, J. Dobbins, X. Liu, and K. Smolenski, Rev. Sci. Instrum. **85**, 093306 (2014).
[15]H. Gruszka and H. Moscicka-Grzesiak, IEEE Trans. Electr. Insul. **EI-20**, 705 (1985).
[16]C. K. Sinclair *et al*., Phys. Rev. Spec. Top.: Accel. Beams **10**, 023501 (2007).
[17]"Electropolishing," http://www.ableelectropolishing.com.
[18]M. BastaniNejad *et al*., Nucl. Instrum. Methods A **762**, 135 (2014).
[19]K. Halbach, Lawrence Livermore National Laboratory Technical Report No. UCRL-17436, 1967.
[20]M. BastaniNejad *et al*., Phys. Rev. Spec. Top. Accel. Beams **15**, 083502 (2012).
[21]B. Bhushan, J. C. Wyant, and J. Meiling, Wear **122**, 301 (1988); V. Filip, D. Nicolaescu, M. Tanemura, and F. Okuyama, Ultramicroscopy **89**, 39 (2001).
[22]C. Xu, H. Tian, C. E. Reece, and M. J. Kelley, Phys. Rev. Spec. Top.: Accel. Beams **15**, 043502 (2012).
[23]C. Xu, C. E. Reece, and M. J. Kelley, Appl. Surf. Sci. **274**, 15 (2013).
[24]H. Tomaschke and D. Alpert, J. Appl. Phys. **38**, 881 (1966).
[25]H. Chen *et al*., Phys. Rev. Lett. **109**, 204802 (2012).
[26]R. Huang, D. Filippetto, C. F. Papadopoulos, H. Qian, F. Sannibale, and M. Zolotorev, Phys. Rev. ST Accel. Beams **18**, 013401 (2015).
[27]O. Y. Kolesnychenko, O. I. Shklyarevskii, and H. van Kempen, Physica B **284**, 1257 (2000).
[28]J. Biersack, J. P. Ziegler, and M. D. Ziegler, "Interactions of ions with matter" http://www.srim.org, 1985.